Structure and Conformation of Spin-Labeled Amino Acids in Frozen Solutions Determined by Electron Nuclear Double Resonance. 1. Methyl *N*-(2,2,5,5-Tetramethyl-1-oxypyrrolinyl-3-carbonyl)-L-alanate, a Molecule with a Single Preferred Conformation[1a]

Devkumar Mustafi, Joseph R. Sachleben, Gregg B. Wells,[1b] and Marvin W. Makinen*

Contribution from the Department of Biochemistry and Molecular Biology, The University of Chicago, Cummings Life Science Center, 920 East 58th Street, Chicago, Illinois 60637.
Received June 7, 1989

Abstract: The conformation of methyl L-alanate acylated at the amino nitrogen position with the nitroxyl spin-label 2,2,5,5-tetramethyl-1-oxopyrroline-3-carboxylic acid has been determined by electron nuclear double resonance (ENDOR) spectroscopy and computer-based molecular modeling. ENDOR resonance absorptions for each class of protons of the amino acid moiety were well resolved under conditions of very low modulation depth (6–8 kHz) of the radio frequency field and were assigned on the basis of selective deuteriation. From analysis of the dependence of the ENDOR spectra on $\mathbf{H}_0$, we have identified the maximum and minimum ENDOR shifts of each class of protons, which correspond to their principal hyperfine coupling (hfc) components. Under the point-dipole approximation, the dipolar hfc components yielded estimates of the electron–nucleus separations with less than a 4% error based on the ENDOR line widths. Computer-based torsion angle search calculations were carried out in order to determine the conformational space compatible with hard-sphere nonbonded constraints and with the ENDOR-determined electron–nucleus separations. The *N*-acyl peptide linkage of the spin-label with the alanyl moiety is characterized by a planar trans conformation and is rigidly constrained. Three conformations of the methyl carboxylate ester group were identified as compatible with ENDOR-determined distance constraints and were equivalent to conformations of peptides in right-handed α-helical, polyproline II, and 2_7 ribbon structures. Potential energy calculations indicated that at least 90% of the molecules in solution at the freezing temperature of methanol have a methyl carboxylate conformation similar to that of a right-handed α-helix.

The unpaired electron spin of paramagnetic molecules interacts with magnetic nuclei in its immediate environment, producing shifts in their resonance frequencies that are dependent on anisotropic dipolar and isotropic contact hyperfine (hf[2]) interactions. The dipolar contribution depends upon the distance of the nuclear spin from the paramagnetic site and the orientation of the static magnetic field with respect to magnetic axes in the molecule. Electron nuclear double resonance (ENDOR[2]) spectra of polycrystalline samples or frozen solutions of paramagnetic molecules, obtained by partially saturating an EPR transition and simultaneously sweeping the sample with a radio frequency field, can be analyzed to yield the dipolar contributions and to determine relative nuclear coordinates. In certain favorable cases dependent on anisotropy in the *g*, hf, or fine structure interactions, single-crystal-like ENDOR spectra can be obtained by setting the static laboratory magnetic field $\mathbf{H}_0$ to the so-called turning points in the EPR spectrum.[3] While it has been frequently assumed that the ENDOR shifts of the nuclear transitions are symmetrically spaced about the Larmor frequency of the nucleus, the insightful analysis of Kreilick and co-workers[4] on the mathematical relationships describing the magnetic interactions responsible for ENDOR of polycrystalline systems shows that ENDOR shifts may be asymmetrically distributed under conditions of significant *g* anisotropy and that the ENDOR spectra then might not yield to meaningful analysis. However, in the absence of significant *g* anisotropy, the ENDOR splittings are to first order symmetrically spaced about the Larmor frequency, and under such conditions we have shown how ENDOR spectroscopy can be applied to polycrystalline or disordered systems to define molecular structure with an accuracy approaching that obtained by X-ray diffraction methods. In these studies we have assigned the coordination and solvation structures of Gd^{3+} and VO^{2+} complexes[5a,b] and the molecular geometry of nitroxyl spin-labeled fluoroanilides[5c] in frozen solutions. These systems represent molecules with essentially rigid, fixed geometries. In the present series of studies we address the problem of molecular conformational flexibility.

The nitroxyl free-radical species known as spin-labels are chemically stable and magnetically well-behaved, and they have been widely employed in biophysical studies as spectroscopic probes of macromolecular structure.[6] We have shown that ENDOR spectroscopy of nitroxyl spin-labels provides a general method of structure determination of molecules in frozen solutions through measurement of electron–nucleus distances in the 5–11-Å range with an accuracy that is exceeded only by that afforded by single-crystal diffraction methods.[5c] In the present and accompanying publication[7] we report the results of detailed ENDOR and molecular modeling studies of methyl esters of L-alanine and L-tryptophan acylated at the amino nitrogen position with the nitroxyl free radical 2,2,5,5-tetramethyl-1-oxypyrroline-3-carboxylic acid. For these spin-labeled amino acid derivatives, the ENDOR-determined distances, obtained with line width based uncertainties of less than 4%, provide an incisive set of constraints on computer-based torsion angle calculations to define sterically allowed conformational space and to assign rotamer structure and

(1) (a) This work was supported by a grant from the National Institutes of Health (GM 21900). (b) Supported in part by an MSTP Training Grant from the National Institutes of Health (GM 07281).

(2) The following abbreviations are used: EPR, electron paramagnetic resonance; ENDOR, electron nuclear double resonance; hf, hyperfine; hfc, hyperfine coupling; NMR, nuclear magnetic resonance; rf, radio frequency.

(3) (a) Rist, G. H.; Hyde, J. S. *J. Chem. Phys.* **1970**, *52*, 4633–4643. (b) Schweiger, A. *Struct. Bonding (Berlin)* **1982**, *51*, 1–28.

(4) (a) Hurst, G. C.; Henderson, T. A.; Kreilick, R. W. *J. Am. Chem. Soc.* **1985**, *107*, 7294–7299. (b) Henderson, T. A.; Hurst, G. C.; Kreilick, R. W. *J. Am. Chem. Soc.* **1985**, *107*, 7299–7303.

(5) (a) Yim, M. B.; Makinen, M. W. *J. Magn. Reson.* **1986**, *70*, 89–105. (b) Mustafi, D.; Makinen, M. W. *Inorg. Chem.* **1988**, *27*, 3360–3368. (c) Wells, G. B.; Makinen, M. W. *J. Am. Chem. Soc.* **1988**, *110*, 6343–6352.

(6) (a) McConnell, H. M.; Gaffney-McFarland, B. *Q. Rev. Biophys.* **1970**, *3*, 91–136. (b) Berliner, L. J., Ed. *Spin-Labeling: Theory and Applications*; Academic Press: New York, 1976; p 592. (c) Jost, P. C.; Griffith, O. H. *Methods Enzymol.* **1978**, *49*, 369–418.

(7) Wells, G. B.; Mustafi, D.; Makinen, M. W. *J. Am. Chem. Soc.*, following article in this issue.

0002-7863/90/1512-2558$02.50/0

molecular conformation. In the present paper we illustrate the general approach for structure analysis by this method and demonstrate that the spin-labeled compound methyl *N*-(2,2,5,5-tetramethyl-1-oxypyrrolinyl-3-carbonyl)-L-alanate exhibits one preferred conformation in solution. In the accompanying paper[7] we demonstrate that the corresponding methyl L-tryptophanate analogue is conformationally flexible, with rotamer structure depending on solvent environment. The results are in excellent agreement with X-ray diffraction studies of corresponding amino acid derivatives crystallized under similar solvent conditions and define structure at a level of resolution that has not been achieved hitherto by any other physical method applied to molecules in solution.

Experimental Procedures

General Materials. Organic solvents were freshly distilled prior to use. All reagents were of analytical reagent grade unless otherwise described. Deionized distilled water was used throughout.

2,2,5,5-Tetramethyl-1-oxypyrroline-3-carboxylic Acid. This spin-label was synthesized according to Rozantsev[8] from 4-oxo-2,2,6,6-tetramethylpiperidine monohydrate (Aldrich Chemical Co., Inc., Milwaukee, WI 53233; mp 210–212 °C with decomposition). Anal. Calcd (Found): C, 58.68 (58.40); H, 7.66 (7.77); N, 7.60 (7.54); O, 26.06 (25.73). Alternatively, the spin-label was purchased from Molecular Probes (Eugene, OR 97402). Similarly, 2,2,5,5-($^2H_{12}$)tetramethyl-1-oxy-4-(^2H)pyrroline-3-carboxylic acid was synthesized from 4-oxo-2,2,6,6-($^2H_{17}$)tetramethylpiperidine (98% deuteriated, MSD Isotopes, St. Louis, MO 63116) with use of ($^2H_4$)acetic acid (99.4%) and perdeuteriated ammonium hydroxide ($N^2H_4O^2H$, 99%) obtained from Cambridge Isotope Laboratories, Inc. (Woburn, MA 01801). NMR analyses of the starting deuteriated piperidine derivative carried out with a Bruker 270-MHz spectrometer indicated ≥96% deuteriation. Characterization of the deuteriated spin-label product according to melting point and elemental analysis yielded results equivalent to those obtained for natural-abundance materials.

Methyl L-Alanate Hydrochloride. To 6 mL of methanol (Aldrich Gold Label, 99.9%) was added 0.15 g of L-alanine (1.68×10^{-3} mol, Aldrich 99%). The suspension was cooled to 0 °C and 0.94 mL of doubly distilled, colorless thionyl chloride (1.28×10^{-2} mol, Aldrich, Gold Label, 99%) was added dropwise with stirring. Then 0.12 mL of H_2O (6.4×10^{-3} mol) was added, whereupon the alanine became soluble and esterification proceeded under acid catalysis. The reaction mixture was stirred for 24 h at room temperature and the solvent removed in vacuo. The residue was repeatedly washed with small volumes (2 mL) of methanol followed by solvent removal in vacuo and recrystallization from methanol–acetone (mp 111–112 °C). Yields of methyl L-alanate hydrochloride were repeatedly in excess of 90%. Anal. Calcd (found): C, 34.42 (33.95); H, 7.22 (7.13); N, 10.03 (9.85). The 270-MHz NMR spectrum showed the following for the product dissolved in ($^2H_4$)methanol: δ 1.54 (3 H, d, CH_3), 3.85 (3 H, s, OCH_3), 4.10 (1 H, q, CH); the amine hydrogens having exchanged with solvent.

The corresponding methyl ester derivatives were synthesized by the same procedure from the following deuteriated analogues of L-alanine (obtained from MSD Isotopes): L-($^2H_4$)ananine (98.8%), L-2-(^2H)alanine (98%), and L-3,3,3-($^2H_3$)alanine (98%). Elemental analysis and NMR spectra showed products of purity comparable to natural-abundance materials with the appropriate NMR line-splitting patterns.

Methyl *N*-(2,2,5,5-Tetramethyl-1-oxypyrrolinyl-3-carbonyl)-L-alanate (I). The series of natural-abundance and specifically deuteriated analogues of spin-labeled methyl L-alanate employed in this investigation are illustrated in Figure 1. The following procedure for the synthesis of I was developed in order to optimize yield, particularly for application to expensive deuteriated analogues, and to allow facile separation of the unreacted spin-label starting compound from the N-acylated ester product. To 10 mL of dry methylene chloride (HPLC reagent, Baker Chemical Co., Inc., Phillipsburg, NJ 08865) containing 0.35 g of carbonyl-1,1′-diimidazole (2.15×10^{-3} mol, Aldrich) was added 0.40 g of 2,2,5,5-tetramethyl-1-oxypyrroline-3-carboxylic acid (2.15×10^{-3} mol) followed by stirring at room temperature for 30 min. Methyl L-alanate hydrochloride (0.20 g, 1.43×10^{-3} mol) and multiply distilled triethylamine (0.20 mL, 1.43×10^{-3} mol) were added, and the reaction mixture was stirred for 48 h at room temperature. The methylene chloride solution was extracted with 0.05 N HCl, 5% (w/v) $NaHCO_3$, and water and dried over $MgSO_4$, whereupon the solvent was removed in vacuo. This procedure yielded the product as yellow crystals, generally with

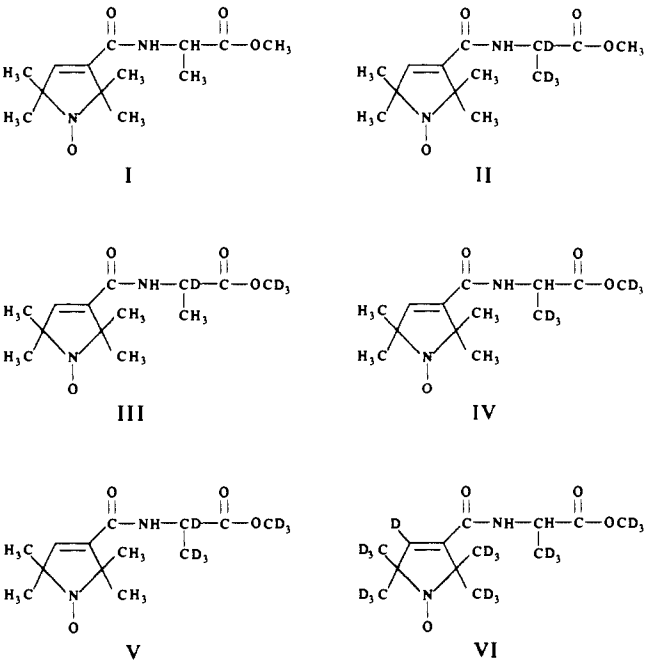

Figure 1. Illustration of the chemical-bonding structure of methyl *N*-(2,2,5,5-tetramethyl-1-oxypyrrolinyl-3-carbonyl)-L-alanate (I) and of the specifically deuteriated analogues II–VI employed in this study.

greater than 50% yield. Occasionally, when the product remained an oil, 2 mL of acetone was added and then removed by rotary evaporation to yield yellow crystals (mp 126–130 °C). Anal. Calcd (Found): C, 57.98 (57.62); H, 7.86 (8.04); N, 10.40 (10.26).

Corresponding spin-labeled analogues of the specifically deuteriated compounds II–VI in Figure 1 were synthesized by the same procedure. Comparable results were obtained for deuteriated analogues of L-alanine with respect to melting point determination and elemental analysis.

EPR and ENDOR. Spectra were recorded at 40 K with an X-band Bruker ER200D spectrometer equipped with an Oxford Instruments ESR10 liquid helium cryostat and a Bruker digital ENDOR accessory, as previously described.[5] ENDOR spectra were recorded in the first-derivative absorption mode with 1.28-mW incident microwave power, 12.5-kHz frequency modulation of the rf field, and 50-W rf power with less than 10-kHz modulation depth of the rf field. The latter is a particularly important condition to achieve the spectral resolution described in this investigation for resonances within 0.5 MHz of their respective free nuclear frequencies. The static laboratory magnetic field was not modulated for ENDOR. The spin-labeled derivatives were dissolved to a concentration of 5×10^{-3} M in ($^2H_4$)methanol (Cambridge Isotope Laboratories, Inc., >99.8%) for spectroscopic studies.

Molecular Modeling. Atomic coordinates of I for modeling studies were derived on the basis of molecular fragments. The atomic numbering scheme is shown for purposes of discussing molecular modeling results.

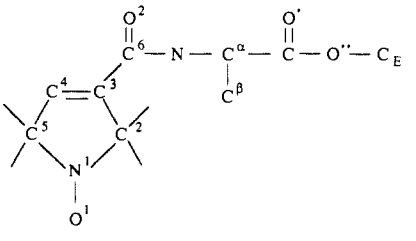

Since the methyl groups bonded to the C(2) and C(5) atoms of the pyrrolinyl spin-label do not directly affect the description of modeling results, they are not designated in the numbering scheme for purposes of brevity. The atomic coordinates of the non-hydrogen atoms of the spin-label moiety, including the carbon, oxygen, and nitrogen of the amide bond, were taken from the X-ray crystallographically defined structure of 2,2,5,5-tetramethyl-1-oxypyrroline-3-carboxamide,[9] and the positions of the non-hydrogen atoms of the methyl L-alanate moiety were based on the X-ray-defined structure of the C-terminal alanyl residue of methyl L-alanyl-*O*,*N*-dimethyl-L-tyrosyl-L-alanate.[10] The C(3), C(6),

(8) Rozantsev, E. G. *Free Nitroxyl Radicals*; Plenum Press: New York, 1970; Chapter 9, pp 203–246.

(9) Turley, J. W.; Boer, F. P. *Acta Crystallogr., Sect. B* **1972**, *28*, 1641–1644.

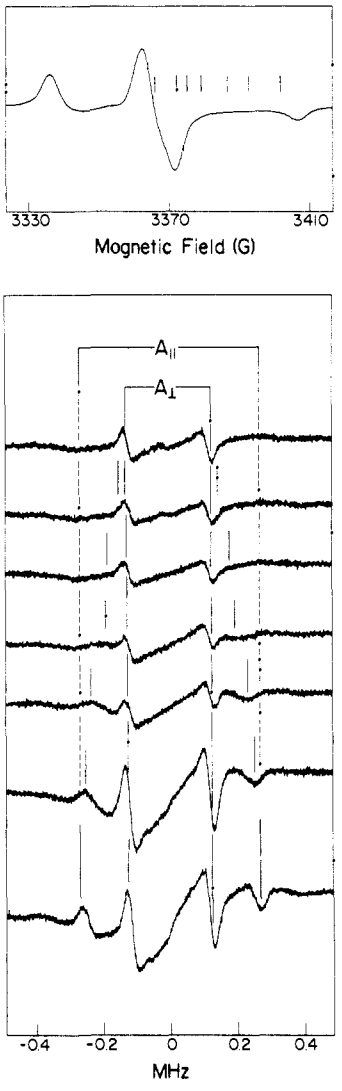

Figure 2. Proton ENDOR spectra of the H^{α} of IV in ($^2H_4$)methanol as a function of magnetic field settings in the EPR spectrum. The descending order of the ENDOR spectra in the lower panel corresponds to the H_0 settings indicated by the right-to-left series of lines in the top panel illustrating the EPR spectrum. The ENDOR absorption features are indicated in each spectrum and are equally spaced about the free proton frequency. The minimum and maximum ENDOR splittings that correspond to two principal hfc components $A_{\parallel}$ and $A_{\perp}$ are identified in the stick diagram.

O(2), and N atoms of the carboxamide group of the spin-label were least-squares superpositioned onto the C^{α}, C, O, and N atoms of the tyrosinyl–alanate peptide bond of the reference derivative to construct the spin-labeled alanine analogue. The root-mean-square deviation of the four spin-label atoms from their positions in the reference peptide was 0.032 Å. Positions of hydrogen atoms were calculated for idealized geometries with C–H and N–H bond lengths of 1.08 and 1.00 Å, respectively.

Analysis of molecular models according to distance constraints obtained from ENDOR studies was carried out with use of the program package SYBYL[11] running on an Evans & Sutherland PS390 molecular graphics system interfaced to a host VAX3500 computer. The basic elements and philosophy underlying the use of this program package, particularly for the calculation of molecular conformation, have been described by Naruto et al.,[12a] and parameters for van der Waals contact radii used were those of Iijima et al.[12b] With this program package, a systematic conformational analysis was carried out with SEARCH, which checks for van der Waals contacts among nonbonded atoms by scanning all possible torsional angles around the rotatable bonds and identifies within the van der Waals allowed conformational space those conformations that are compatible with specified ENDOR distances together with their respective uncertainties as added constraints.

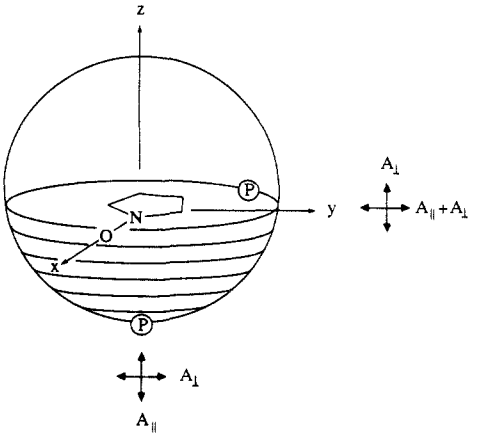

Figure 3. Schematic illustration of the relationships of the symmetry axes of the nitroxide molecule to the principal axes of the g matrix and of the hf interaction matrix of nearby protons. Each circle represents the field orientation within the g axis system that is selected for saturation in the ENDOR experiment. Relative positions of protons in the molecular x,y plane or on the symmetry z axis are also indicated. The diagram also illustrates the principal hfc components that are detected for protons according to whether H_0 is aligned parallel to or perpendicular to the z axis.

Characteristics of ENDOR Spectra of Nitroxyl Spin-Labels at Selected Molecular Orientations

ENDOR transitions occur as a result of the electron and nuclear spins interacting with simultaneously applied microwave and rf fields. The first-order ENDOR transition frequencies[4a] for a nucleus are given by eq 1

$$\nu_{\pm} = \left[\sum_{i=1}^{3}\left[\frac{m_S}{g_e}\left(\sum_{j=1}^{3} g_j l_j A_{ji}\right) - l_i \nu_n\right]^2\right]^{1/2} \quad (1)$$

where the l_i are the direction cosines of $\mathbf{H}_0$ in the molecular axis system, A_{ji} is the orientation-dependent value of the hf coupling, ν_n is the nuclear Larmor frequency, m_s is the electron spin quantum number, and $g_e^2 = \sum_{j=1}^{3} l_i^2 g_i^2$. In systems of low g anisotropy, as for nitroxyl spin-labels,[13-16] the ENDOR transition frequencies are symmetric about the nuclear Larmor frequency. The observed hf couplings A are given by eq 2 as a function of the electron–

$$A = \frac{g_e|\beta_e|g_n|\beta_n|}{hr^3}(3\cos^2\alpha - 1) + A_{iso} \quad (2)$$

nucleus separations r and the dipolar angles α. The other quantities in eq 2 have their classical definitions.[4,5] Since g_e remains essentially constant over the range of $\mathbf{H}_0$ for a spectral scan of a nitroxyl spin-label, eq 2 implies dependence of the value of A on the angle α. These relationships are illustrated in Figure 2 by the series of ENDOR spectra of IV. The ENDOR features in Figure 2 belong only to H^{α} since the amide proton has been exchanged with solvent deuterons. When the magnetic field is

(10) Bates, R. B.; Hruby, V. J.; Kriek, G. R. *Acta Crystallogr., Sect. B* **1979**, *35*, 188–191.
(11) Marshall, G. R., personal communication. Detailed information on the use of this program package can be obtained from Tripos Associates, Inc., 1600 S. Hanley Road, St. Louis, MO 63144.
(12) (a) Naruto, S.; Motoc, J.; Marshall, G. R.; Daniels, S. B.; Sofia, M. J.; Katzenellenbogen, J. A. *J. Am. Chem. Soc.* **1985**, *107*, 5262–5270. (b) Iijima, H.; Dunbar, J. B., Jr.; Marshall, G. R. *Proteins: Struct., Funct., Genet.* **1987**, *2*, 330–339.
(13) Griffith, O. H.; Cornell, D. W.; McConnell, H. M. *J. Chem. Phys.* **1965**, *43*, 2909–2910.
(14) Capiomont, A.; Chion, B.; Lajzerowicz-Bonneteau, J.; Lemaire, H. *J. Chem. Phys.* **1974**, *60*, 2530–2535.
(15) Brustolon, M.; Maniero, A. L.; Carvaja, C. *Mol. Phys.* **1984**, *51*, 1269–1281.
(16) Lee, S.; Ames, D. P.; Putnam, J. M. *J. Magn. Reson.* **1982**, *49*, 312–321.
(17) (a) For these calculations we have employed the ENDOR spectral simulation program SPOTELI[17b] supplied by Professor B. M. Hoffman (Department of Chemistry, Northwestern University, Evanston, IL 60201). (b) Hoffman, B. M.; Gurbiel, R. J. *J. Magn. Reson.* **1989**, *82*, 309–317.

set to either the high-field or low-field turning points in the EPR spectrum, a single molecular orientation can be selected such that $\mathbf{H}_0$ is aligned perpendicularly to the pyrrolinyl ring.[5c] The corresponding observed hf splitting is illustrated in the topmost ENDOR spectrum. The subsequent ENDOR spectra illustrated in descending order correspond to $\mathbf{H}_0$ settings, approaching and finally coinciding with the center of the prominent, central EPR absorption feature. The splitting of the innermost pair of ENDOR features does not change perceptibly with change in $\mathbf{H}_0$ while the splitting of the outermost pair of features gradually increases and reaches a maximum value.

The ENDOR splittings in Figure 2 are readily explained with the aid of Figure 3. Because of the very low g anisotropy of the nitroxyl group, we assume to first order that the principal magnetic axes of the $\mathbf{g}_e$ matrix and the hf interaction matrix are concident.[14,15] Figure 3 illustrates schematically the expected pattern of observed ENDOR splittings as a function of the position of the proton and the orientation of $\mathbf{H}_0$ with respect to the molecular plane. When $\mathbf{H}_0$ is aligned parallel to g_{zz} and, therefore, perpendicularly to the molecular plane, the $A_\parallel$ hfc component of a proton located along the symmetry axis or the $A_\perp$ hfc component of a proton located near or in the molecular plane are observed. As $\mathbf{H}_0$ is set to correspond closer and closer to an orientation in and finally parallel to the molecular plane, ENDOR absorption due to the $A_\perp$ hfc component of a proton in the molecular plane is detected together with the absorption due to its $A_\parallel$ hfc component. On this basis, if the topmost ENDOR spectrum in Figure 2 belonged to an axially located proton, the parallel hfc component would decrease monotonically in intensity while the perpendicular hfc component would gradually increase in intensity as $\mathbf{H}_0$ is set closer to the central region of the EPR spectrum. The innermost pair of features in Figure 2 is observed with $\mathbf{H}_0$ perpendicular to the molecular plane, and the value of this splitting is independent of the $\mathbf{H}_0$ setting. The observation that the value of this splitting is less than the largest splitting observed with $\mathbf{H}_0$ in the molecular plane identifies H^α as lying in or nearly coincident with the plane of the pyrrolinyl ring. Thus, when the central feature of the EPR spectrum of a nitroxyl spin-label is saturated for ENDOR, both the parallel and perpendicular hfc components of a proton in the molecular plane will be observed while only the perpendicular hfc component will be observed when the low-field or high-field EPR feature is saturated. In this manner, selection of molecular orientation can be achieved with identification of both parallel and perpendicular hfc components.

Our assignment of the principal components of H^α according to Figures 2 and 3 is confirmed by calculation of the field dependence of the principal components of the hf matrix illustrated in Figure 4, which compares the $\mathbf{H}_0$ dependence of the ENDOR shift of H^α in compound IV measured experimentally and calculated according to eq 1. When $\mathbf{H}_0$ is applied to g_{zz} at the high-field or low-field edge of the EPR absorption spectrum, the intensity function, as first described by Rist and Hyde,[3a] is single-crystal-like with ENDOR transitions at $\nu_\pm = \nu_n \pm |A_\perp|/2$. As $\mathbf{H}_0$ is gradually shifted from the high- or low-field edge toward the central region of the EPR spectrum, a second pair of absorption features is observed for which the ENDOR shift increases smoothly until a maximum value is reached, the other two absorptions remaining fixed at their originally observed transition frequencies. The maximum ENDOR shift of the outer pair of resonance features occurs when $\mathbf{H}_0$ is applied within the central feature of the EPR spectrum and is coincident with g_{xx} and g_{yy}.

We have also calculated the field-dependent hfc components of H^α under the condition of $A_\parallel \| g_\parallel$. In this case the maximum calculated hfc occurs with $\mathbf{H}_0$ at the low- or high-field edge of the EPR spectrum. The splitting decreases smoothly to its minimum value when $\mathbf{H}_0$ is at the central region of the EPR spectrum. For a proton in a position intermediate between those illustrated in Figure 3, the calculated maximum hfc component is found when $\mathbf{H}_0$ is set to a value between the central absorption region and the low- or high-field extremes of the EPR spectrum. The appearance of the two pairs of ENDOR absorptions according to $\mathbf{H}_0$ setting, as shown in Figure 4, thus, assigns the orientation

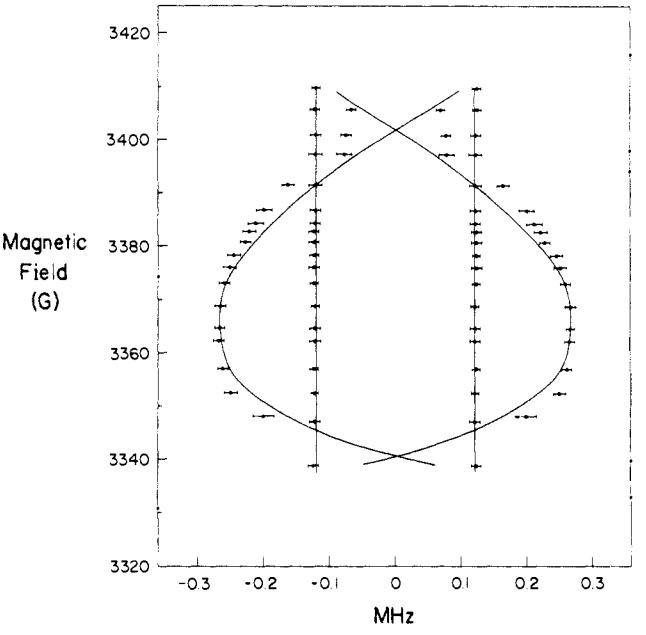

Figure 4. Magnetic field dependence of the ENDOR shift of H^α of compound IV. Experimentally observed ENDOR absorption features with $\mathbf{H}_0$ as illustrated in Figure 2 are indicated by points with error bars drawn according to the uncertainties in ENDOR line widths. Solid lines are calculated[17] according to eq 1 with $g_\parallel = 2.0026$, $g_\perp = 2.0076$ under the condition $A_\parallel \perp g_\parallel$. The parallel ENDOR resonance absorptions exhibit larger deviations from calculated values at the high-field and low-field regions of the plot than in the central region. These larger deviations are ascribable to a greater uncertainty in assigning the position of parallel resonance absorptions with closely overlapping perpendicular features, as seen in Figure 2.

of the hf axes with respect to the plane of the nitroxide ring. While the $\mathbf{H}_0$ dependence of the ENDOR spectrum of IV in Figure 2 identifies the position of H^α as coincident with the molecular plane, the calculated field dependence of the hfc components confirms our assignment of the direction of the principal components of A with respect to the molecular plane of the nitroxyl spin-label.

Results

A. Proton ENDOR of Spin-Labeled Methyl L-Alanate. 1. Assignment of ENDOR Resonance Features by Deuteriation. In Figure 5 are illustrated proton ENDOR spectra of VI at two different settings of $\mathbf{H}_0$. For these spectra the spin-labeled derivative was first mixed in ($^2H_4$)methanol and rapidly frozen in liquid nitrogen for spectral data collection. After spectral recording, the frozen sample was thawed and refrozen. Because of proton exchange of the amide group with solvent, this procedure allows assignment of the resonance features of the amide proton and their separate identification from the absorption features due to H^α. From both sets of spectra, two pairs of resonance features are attributed to the parallel and perpendicular hfc components of the amide proton. The resonance features that remain after thawing of the rapidly frozen mixture belong to H^α. The splittings for H^α are identical with the maximum and minimum values of the hfc components shown in Figure 2.

Figure 6 illustrates proton ENDOR spectra of compounds I–V with $\mathbf{H}_0$ at setting B. For each spectrum, sufficient time after mixing the derivative in ($^2H_4$)methanol was allowed to ensure complete exchange of the amide proton with solvent. The overlapping features in the spectrum of I illustrate the need to identify specific resonance features of each class of protons through use of deuteriated analogues. The spectra in Figure 6 with the $\mathbf{H}_0$ setting corresponding to the "isotropic approximation"[5c] yield both the perpendicular and the parallel hfc components of each class of protons. The origins of the ENDOR absorptions are directly assigned on the basis of deuteriation.

The ENDOR features of the hydrogens attached to C^β are of added interest since close inspection of the spectra revealed two perpendicular hfc components and two closely overlapping parallel

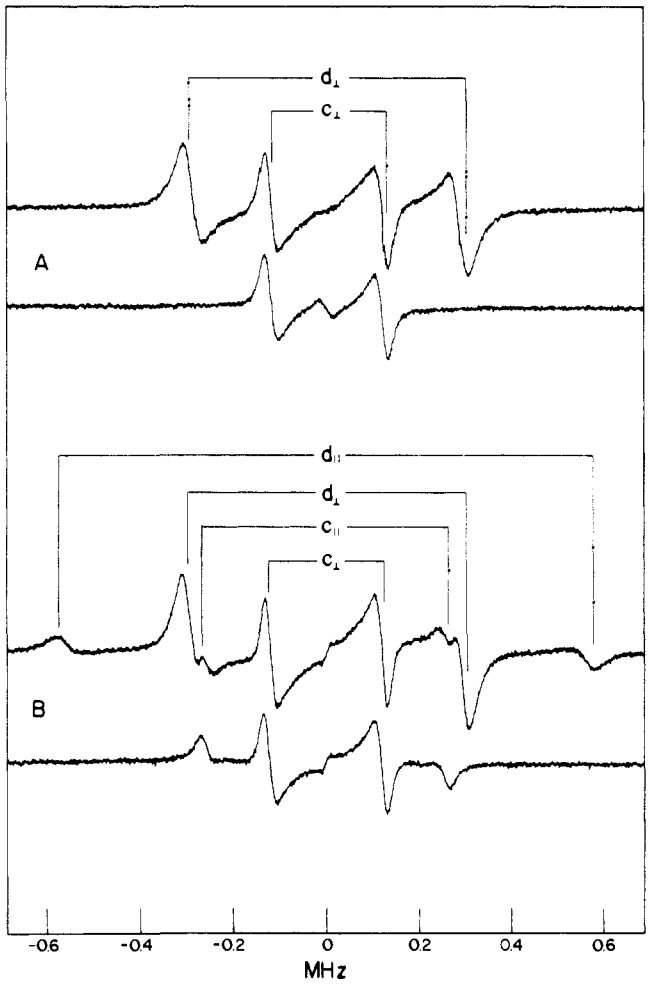

Figure 5. Proton ENDOR spectra of VI in ($^2H_4$)methanol. Letters A and B correspond to H_0 settings at the low-field edge and the central region of the EPR spectrum, respectively, that were saturated for ENDOR. Microwave saturation at position A selects molecules with $m_I = +1$ for ENDOR with $\mathbf{H}_0$ perpendicular to the plane of the five-membered ring, while microwave saturation at setting B selects all molecular orientations with $m_I = 0$.[5c] For each field setting, the bottom spectrum was taken after exchanging H^N with solvent deuterium. The ENDOR splittings of H^α and H^N are identified in the stick diagram by $c_\parallel$, $c_\perp$ and $d_\parallel$, $d_\perp$, respectively, for the two principal hfc components.

absorptions. Identical splittings and intensities were observed for III dissolved in perdeuteriated chloroform–toluene. Since the conformation of alanine derivatives is dependent on solvent polarity,[18] this observation suggests that only one conformation of the spin-labeled amino acid obtains and is responsible for both sets of absorptions. With increasing temperature over the 40–100 K range, it was observed that two features labeled $b_\perp'$ and $b_\perp''$ broadened and finally coalesced. Since the matrix remains solid at these temperatures, the absorptions would have remained separated if they derived from two different conformations. We, therefore, suggest that the coalescence of the absorption features is due to the onset of rotation of the methyl group about the C^α–C^β bond at higher temperatures. Studies of the dynamics of methyl groups in free-radical molecules have shown the onset of methyl rotation near temperatures of 80 K.[19]

(18) (a) Bystrov, V. F.; Portnova, S. L.; Tsetlin, V. I.; Ivanov, V. T.; Ovchinnikov, Yu. A. *Tetrahedron* **1969**, *25*, 493–515. (b) Neel, J. *Pure Appl. Chem.* **1972**, *31*, 201–225. (c) Crippen, G. M.; Yang, J. T. *J. Phys. Chem.* **1974**, *78*, 1127–1130. (d) Madison, V.; Kopple, K. D. *J. Am. Chem. Soc.* **1980**, *102*, 4855–4863. (e) Mezei, M.; Mehrotra, P. K.; Beveridge, D. L. *J. Am. Chem. Soc.* **1985**, *107*, 2239–2245.

(19) (a) Miyagawa, I.; Itoh, K. *J. Chem. Phys.* **1962**, *36*, 2157–2163. (b) Wells, J. W.; Box, H. C. *J. Chem.* Phys. **1967**, *46*, 2935–2938. (c) Brustolon, M.; Cassol, T.; Micheletti, L.; Segre, U. *Mol. Phys.* **1986**, *57*, 1005–1014. (d) Brustolon, M.; Cassol, T., Micheletti, L.; Segre, U. *Mol. Phys.* **1987**, *61*, 249–255.

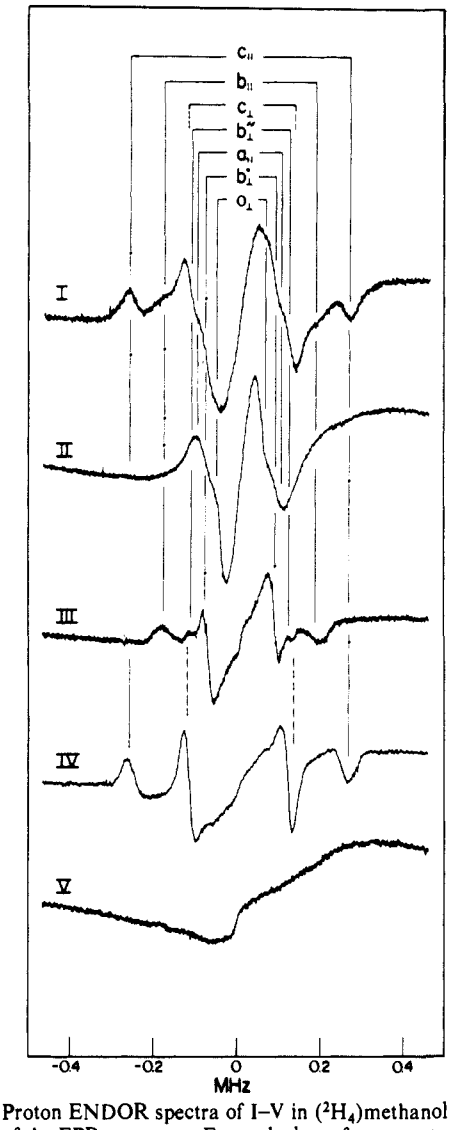

Figure 6. Proton ENDOR spectra of I–V in ($^2H_4$)methanol with H_0 at position B of the EPR spectrum. For each class of protons, two line pairs are seen equally spaced about the free proton frequency and are assigned to parallel and perpendicular hfc components. For H^β protons two perpendicular hfc components are observed but their corresponding parallel components are closely overlapping and labeled as $b_\parallel$.

Table I. Summary of hfc Components and Estimated Electron–Proton Distances in Methyl *N*-(2,2,5,5-Tetramethyl-1-oxypyrrolinyl-3-carbonyl)-L-alanate

proton type	line pairs[a]		hfc components, MHz					r,[b] Å
			$A_\parallel$	$A_\perp$	A_{iso}	$A_\parallel^D$	$A_\perp^D$	
OCH_3	$a_\parallel$	$a_\perp$	0.204	0.103	0.000	0.204	−0.103	9.19 ± 0.22
CH_3	$b_\parallel''$	$b_\perp''$	0.384	0.237	−0.030	0.414	−0.207	7.30 ± 0.04[c]
CH_3	$b_\parallel'$	$b_\perp'$	0.346	0.173	0.000	0.346	−0.173	7.71 ± 0.06[d]
CH	$c_\parallel$	$c_\perp$	0.525	0.244	0.013	0.513	−0.256	6.76 ± 0.04
NH	$d_\parallel$	$d_\perp$	1.152	0.605	−0.019	1.172	−0.586	5.13 ± 0.02

[a] Line pairs are assigned in Figures 5 and 6. The parallel hfc components for two H^β nuclei are not well resolved in Figure 6; however, values are given according to spectra taken on an expanded scale (data not shown). [b] Uncertainty in frequency of 0.015–0.020 MHz due to the line width of each absorption is included in the calculation of electron–proton distances. [c] Assigned to $H^{\beta 1}$, as discussed in the text, on the basis of the relative intensities of the $b_\perp'$ and $b_\perp''$ ENDOR features. [d] Assigned to the geometric mean of $H^{\beta 2}$ and $H^{\beta 3}$, as discussed in the text.

The spectra in Figure 6 exhibit two sets of resonances that are resolved for the methyl protons of the alanine side chain. The two resonances differ considerably in intensity. Since the resonances are not ascribable to different conformations of the molecule and since we cannot explain why three separate resonances are not resolved, we attribute the more intense $b_\perp'$ resonances to two of the three protons while the weaker $b_\perp''$ resonances

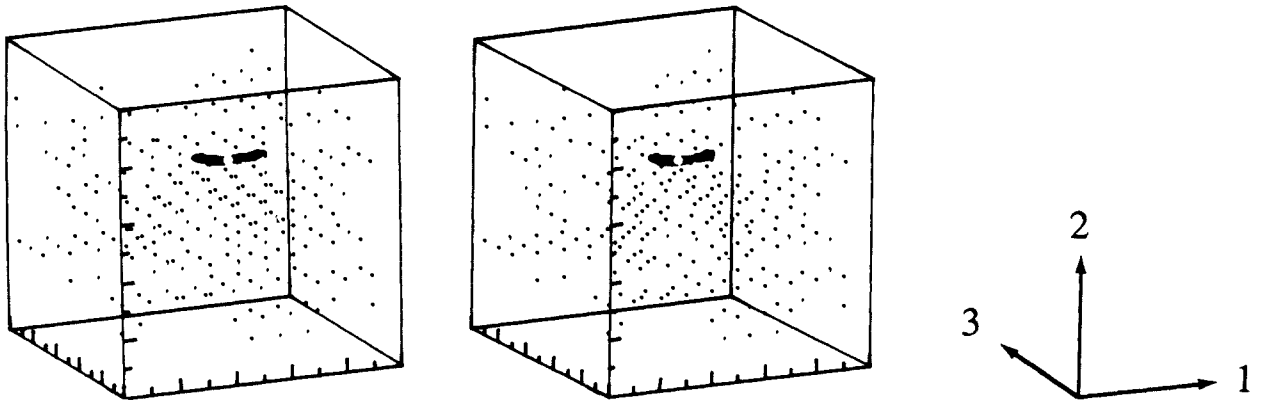

Figure 7. Stereo diagram of the angle map of spin-labeled methyl L-alanate defining the conformation of the molecule from the nitroxyl group to the C^{α} and C^{β} atoms of the alanine moiety. The axes 1–3 represent 0–360° rotation around the N–C^{α}, C(6)–N, and C(3)–C(6) bonds, respectively. Each dot in the cube represents a set of three calculated torsion angles.

are assigned to the third proton of the methyl group. This assignment is consistent with our structural analysis, as shown below.

2. ENDOR-Based Electron–Proton Distances. In Table I we have summarized the observed parallel and perpendicular hfc components of each class of protons of the spin-labeled methyl L-alanate obtained from ENDOR spectra. From the observed maximum and minimum ENDOR shifts that correspond to $A_{\parallel}$ and $A_{\perp}$, respectively, and under the conditions that $A_{iso} \ll A_{\parallel}$ and $A_{\perp}$, then $A_{\parallel}^{D} > 0 > A_{\perp}^{D}$ and the dipolar hfc contributions $A_{\parallel}^{D}$ and $A_{\perp}^{D}$ can be calculated under the constraint $(A_{\parallel} + 2A_{\perp}) = 3A_{iso}$.[5] We have also listed our estimates of the corresponding A_{iso} values and the ENDOR-determined values of r calculated on the basis of eq 2. The results show that the isotropic hfc contribution is essentially negligible, as expected from our earlier study of spin-labeled fluoroanilides.[5c] The calculated distances all show very small uncertainties because of the high resolution of the ENDOR spectra and the relatively narrow line widths of the resonance features through use of specifically deuteriated analogues.

B. Molecular Modeling of Spin-Labeled Methyl L-Alanate. To determine the conformation of spin-labeled methyl L-alanate, we have carried out a computational search of the limits of the torsion angles for rotation around the C(3)–C(6) and C(6)–N bonds within the spin-label acyl moiety and around the N–C^{α}, C^{α}–C^{β}, C^{α}–C, and C–O″ bonds of the methyl alanate moiety. Torsional search calculations were carried out to identify the conformations within nonbonded hard-sphere limits[12b] that are compatible with the electron–proton distances summarized in Table I. The search calculations were applied simultaneously to all bonds indicated above to ensure the "frozen" parts of the molecule did not sterically constrain the allowed range of conformations. For computational purposes the search was performed in 5° increments of torsion angle rotation.

For these calculations the effective electron dipole position $\mathbf{r}_e$ was assigned as discussed earlier[5c] according to the relation $\mathbf{r}_e = \rho_N \mathbf{r}_N + \rho_O \mathbf{r}_O$ where $\rho_N = 0.552$ and was determined on the basis of the isotropic nitrogen hfc measured from the EPR absorption of I in ($^2H_4$)methanol. The value of ρ_N, as discussed later, assigns the effective electron dipole 0.569 Å away from the nitroxyl nitrogen atom along the N–O bond. The ENDOR-determined distance constraints for H^N and H^{α} were applied directly. For the protons of the alanine side chain, the 7.30 ± 0.04 Å constraint belonging to the resonance of weaker intensity was applied to a single proton ($H^{\beta 1}$) while the 7.71 ± 0.06 Å constraint was applied to the calculated geometrical mean position of the other two protons ($H^{\beta 2}$, $H^{\beta 3}$). On the other hand, we have applied the distance constraint of the OCH_3 group to the calculated geometrically averaged position of three methyl protons bonded to a tetrahedral carbon atom. We discuss the results for rotation about each bond separately.

Rotation around the C(3)–C(6), C(6)–N, and N–C^{α} bonds showed that a cis conformation of the peptide bond joining the spin-label moiety to alanine is incompatible with the ENDOR-determined distance constraint of 5.13 ± 0.02 Å to H^N. Simultaneous application of distance constraints to H^N and H^{α} limited the [C(3)–C(6)–N–C^{α}] torsion angle to values between 171° and 201°.[20] While these results are sufficient to assign a planar trans conformation to the peptide bond, further application of the distance constraints to the methyl protons of the alanine side chain restricts the value of this torsion angle to 190 ± 4° (−170 ± 4°). This result is in excellent agreement with the value of −172° of the corresponding dihedral angle of the tyrosinyl–alanine peptide bond of the parent tripeptide,[10] from which atomic coordinates were derived to construct the molecular model of spin-labeled methyl L-alanate. This resultant conformation of the spin-label moiety yielded values of 146 ± 5° and −35 ± 5° for the dihedral angles [C(4)–C(3)–C(6)–O(2)] and [C(4)–C(3)–C(6)–N], respectively, in excellent agreement with the corresponding values of 149° and −31° in the parent tripeptide.[10] Furthermore, a torsion angle search around the C^{α}–C^{β} bond to analyze the conformations of H^{α} with respect to the protons of the alanine side chain showed that application of the H^{α} and H^{β} distance constraints resulted in a value of −70 ± 5° or 156 ± 5° for the [H^{α}–C^{α}–C^{β}–$H^{\beta 1}$] torsion angle. These values are very close to those of −60° and 180° expected for idealized stereochemical relationships.

The results of the torsion angle search calculations are represented by the angle map in Figure 7 and are discussed as a function of the number of ENDOR distance constraints. The low-density dots represent the conformational space allowed by only nonbonded van der Waals interactions. The small region of high-density dots represents the conformational space allowed under application of nonbonded van der Waals constraints together with the distance constraints to H^N and H^{α}. Application of the additional distance constraint to $H^{\beta 1}$ did not change significantly the volume of space calculated for H^N and H^{α} constraints alone. On the other hand, the addition of the fourth distance constraint to the geometrical mean of $H^{\beta 2}$ and $H^{\beta 3}$ reduced sharply the allowed conformational space to a single point represented by the white dot within the volume of high-density dots. On the other hand, torsion angle calculations around the N–C^{α}, C^{α}–C, and C–O″ bonds showed three distinct families of conformations of the methyl carboxylate group compatible with the ENDOR-determined distance of 9.19 ± 0.22 Å to the ester methyl group.

We have illustrated in Figure 8 the single conformation of the spin-label moiety defined by the angle map in Figure 7 together with the three conformations of the ester group. The graphics analysis reveals that the conformation of the molecule from the nitroxyl group to the C^{α} and C^{β} atoms of the alanine moiety is rigidly constrained. The only flexible portion of the molecule is the methyl carboxylate group. The carboxylate group of structure A in Figure 8 is closer to that of a classical *Z* conformation of

(20) The conventions and nomenclature used are those described by the IUPAC–IUB Commission on Biochemical Nomenclature: *Biochemistry* **1970**, *9*, 3471–3479.

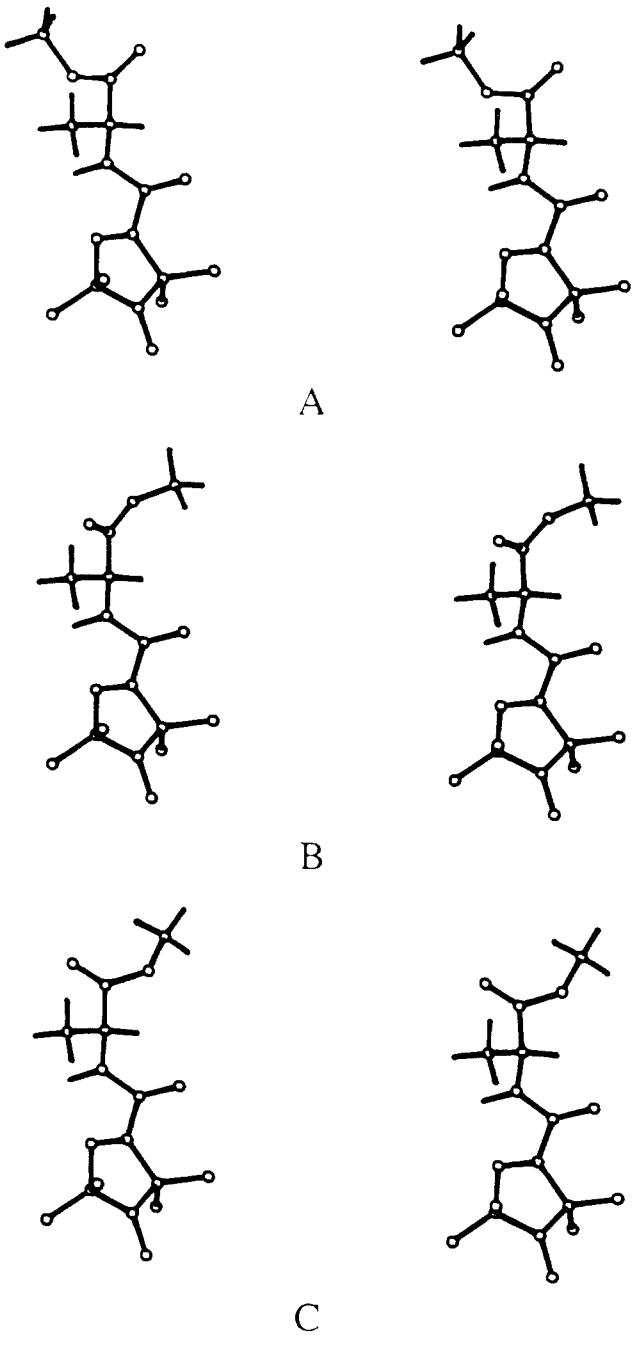

Figure 8. Stereo diagram of three conformations of spin-labeled methyl L-alanate. The conformation of the molecule from the nitroxyl ring to the C^{β} atom of the alanine moiety remains constant for all conformations. The conformations of the methyl ester group A, B, and C correspond to the mean structure of each of the three families of conformers, as listed in Table III. The ENDOR-significant hydrogen positions are shown in addition to the non-hydrogen atoms.

an ester group than are the other two.

Discussion

A. The Effective Position of the Electronic Dipole of the Nitroxyl Group. It has been shown that the unpaired electron of spin-labels is almost entirely localized to the nitroxyl group of the pyrrolinyl ring.[13-15,21] Since the spin density is distributed over both atoms of the nitroxyl group, the measured dipolar hf interaction for a nearby magnetic nucleus must be viewed as a composite interaction of the unpaired spin confined to the oxygen and the nitrogen atoms individually. On this basis, the separate dipolar interactions will depend on the fraction of the total spin density associated with the nitrogen and with the oxygen atom of the nitroxyl group. The distribution of spin density can be directly estimated from the measured isotropic nitrogen hf coupling of the nitroxyl group according to the Karplus-Fraenkel relationship[22] $a_N = \rho_N Q_N + \rho_O Q_O$ where the ρ's represent the individual fractional spin densities associated with the nitrogen and oxygen atoms for the nitroxyl group in methanol. The constants Q_N and Q_O have values of 24.2 and 3.6 G, respectively.[23] Our value of 14.96 ± 0.05 G for a_N estimated from the isotropic nitrogen hfc of I in methanol yields values of 0.552 and 0.448 (±0.028) for ρ_N and ρ_O, respectively.

Since the unpaired electron is distributed over the nitroxyl group, we expect that the hfc component of the dipole-dipole interaction of a given proton will be weighted according to the spin density distribution associated with the nitrogen and oxygen atoms of the nitroxyl group. On this basis we calculate the dipolar coupling components of the ith class of protons according to eq 3 where ρ_j is the spin density at the jth nitroxyl atom estimated

$$A^{D}_{i} = K\sum_{j=1}^{2}\rho_j(3\cos^2\alpha_{ij} - 1)/r^3_{ij} \qquad (3)$$

from the isotropic EPR spectrum, α_{ij} is the angle between the magnetic field and i-j internuclear vector, r_{ij} is the corresponding i-j internuclear distance, and K represents the appropriate constants given in eq 2. Equation 3 requires prior knowledge of proton positions with respect to the atoms of the nitroxyl group, in order to determine the principal hfc components with respect to each nitroxyl atom. Employing the geometry shown in Figure 8, we have compared the values of the dipolar coupling components for each class of protons calculated according to eq 3 with the values of the spectroscopically estimated dipolar hfc components listed in Table I. The largest discrepancy is 3.6% associated with H^N, for which the ENDOR-estimated electron-nucleus separation is 5.13 ± 0.02 Å. As shown in the accompanying publication,[7] the corresponding distance for spin-labeled methyl L-tryptophanate in methanol, estimated as 5.11 ± 0.04 Å, is in excellent agreement. The discrepancy for the other classes of protons is even less, as expected for protons of greater electron-nucleus separations.[5c]

In Table I the values of A_{iso} for each electron-nucleus separation are not greater than the corresponding uncertainties in the observed splittings due to the ENDOR line width. This circumstance means, therefore, that the observed hf couplings are essentially due only to dipolar interactions and provide accurate estimates of the electron-nucleus separations. We have previously evaluated the quantitative limits for application of eq 2 to estimate electron-nucleus separations under the conditions $A_{\parallel}, A_{\perp} \gg A_{iso}$ to show that with nitroxyl spin-labels there is less than a 5% discrepancy in the estimates for electron-nucleus separations greater than 5 Å.[5c] This analysis, as continued in this study, rests on the assignment of the position of the *effective* point dipole of the nitroxyl group according to the estimate of the isotropic nitrogen hfc of the nitroxyl group measured from the EPR absorption spectrum. In recent studies we have had the opportunity to test the limits of these relationships to estimate electron-nucleus separations associated with considerably greater isotropic hf couplings.[24] In particular, the value of A_{iso} for the vinyl proton in the pyrrolinyl ring is -1.81 MHz,[25] and $A_{\perp} > A_{\parallel}$. Estimation of the dipolar hfc components through the relationship $(A_{\parallel} + 2A_{\perp}) = 3A_{iso}$, nonetheless, results in an electron-nucleus separation of 3.78 ± 0.01 Å for the vinyl proton, in excellent agreement with

(21) (a) Davis, T. D.; Christoffersen, R. E.; Maggiora, G. M. *J. Am. Chem. Soc.* **1975**, *97*, 1347-1354. (b) Hayat, H.; Silver, B. L. *J. Phys. Chem.* **1973**, *77*, 72-78.

(22) Karplus, M.; Fraenkel, G. K. *J. Chem. Phys.* **1961**, *35*, 1312-1323.

(23) Cohen, A. H.; Hoffman, B. M. *J. Am. Chem. Soc.* **1973**, *95*, 2061-2062.

(24) (a) Mustafi, D.; Boisvert, W. E.; Makinen, M. W. *Biopolymers* **1990**, *29*, 45-55. (b) Mustafi, D.; Wells, G. B.; Joela, H.; Makinen, M. W. *Free Radical Res. Commun.*, in press.

(25) (a) Kirste, B.; Krüger, A.; Kurreck, H. *J. Am. Chem. Soc.* **1982**, *104*, 3850-3858. (b) Hyde, J. S.; Subczynski, W. K. *J. Magn. Reson.* **1984**, *56*, 125-130.

Table II. Comparison of Dihedral Angles Involving Hydrogen Atoms in the X-ray-Defined Reference Molecular Model[a] and in ENDOR-Constrained Conformations of Methyl *N*-(2,2,5,5-Tetramethyl-1-oxypyrrolinyl-3-carbonyl)-L-alanate

dihedral angle[b]	angle, deg	
	X-ray	ENDOR
[C(3)–C(6)–N–H^N]	8	10 ± 4
[O(2)–C(6)–N–N^N]	−173	−171 ± 4
[H^N–N–C^α–H^α]	−168	−154 ± 12
[H^N–N–C^α–C^β]	−50	−36 ± 12
[H^N–N–C^α–C]	73	88 ± 12
[H^α–C^α–C^β–$H^{\beta 1}$]	−56	−70 ± 5

[a] Idealized hydrogen positions were calculated on the basis of the X-ray defined non-hydrogen atomic coordinates of the reference compound.[10] [b] These dihedral angles are identical for each of the three conformations illustrated in Figure 8.

that of 3.79 Å obtained on the basis of X-ray structural parameters and our assignment of the effective position of the point dipole of the nitroxyl group. We conclude, therefore, that the approach taken in this investigation is logically correct. Since the distribution of spin density can be readily determined experimentally on the basis of the strength of the isotropic nitrogen hfc, as in the present study, this approach is also more direct for purposes of molecular modeling.

B. Conformation of Spin-Labeled Methyl L-Alanate. To assess the accuracy of ENDOR data to assign structural conformation, a molecular model was constructed by superpositioning the C(3), C(6), O(2), and N atoms of 2,2,5,5-tetramethyl-1-oxypyrrolinyl-3-carboxamide[9] onto the C^α, C, O, and N atoms of the terminal L-tyrosinyl-L-alanate peptide bond of the tripeptide reference compound.[10] The ENDOR data provide relative coordinates of each class of hydrogen atoms in the molecule determined with respect to the nitroxyl group and the plane of the five-membered pyrrolinyl ring while the coordinates of only the non-hydrogen atoms are directly determined by X-ray data in the crystallographically defined reference compounds.[9,10] Consequently, we compare corresponding dihedral angle relationships in the crystallographically defined reference compounds to those of the molecular model derived from ENDOR distance constraints applied to idealized hydrogen positions. To this end, the values of the dihedral angles of spin-labeled methyl L-alanate derived from ENDOR data are summarized in Tables II and III and compared to corresponding values of the terminal methyl L-alanate portion of the X-ray-defined reference tripeptide.[10] In Tables II and III the values of the dihedral angles correspond directly to the values obtained on the basis of calculated estimates of r given in Table I while the uncertainties in the values of the dihedral angles are evaluated from the line width based errors. The results of our torsion angle search calculations separate the spin-labeled methyl L-alanate molecule into two parts corresponding (i) to a conformationally rigid portion, extending from the nitroxyl group to the C^β atom of the alanine moiety, and (ii) to the methyl carboxylate group that is found in three distinct conformations.

The values of dihedral angles involving hydrogen atoms in Table II provide the most direct assessment of the quality of the ENDOR data. The values of the [C(3)–C(6)–N–H^N] and [O(2)–C(6)–N–H^N] angles are in excellent agreement with the reference compound and indicate an essentially planar peptide group. Moreover, the tilt of the plane of the peptide group with respect to the pyrrolinyl ring for spin-labeled methyl L-alanate in solution is 32.6° and is essentially identical with that (28.9°) of the carboxamide group for the spin-label molecule in crystals.[9] The values of the [H^N–N–C^α–H^α] and [H^α–C^α–C^β–$H^{\beta 1}$] dihedral angles are particularly noteworthy since they each specify the relative positions of two hydrogens on the basis of ENDOR measurements. Both results are in good agreement with the reference compound and are, furthermore, in close agreement with the respective values of 180° and −60° expected for idealized staggered conformations.

The dihedral angles defined by non-hydrogen atoms are compared in Table III. The angles corresponding to the rigid portion

Table III. Comparison of Dihedral Angles Involving Only Non-Hydrogen Atoms of the X-ray-Defined Reference Molecular Model and of the ENDOR-Constrained Conformations of Methyl *N*-(2,2,5,5-tetramethyl-1-oxypyrrolinyl-3-carbonyl)-L-alanate

dihedral angle	angle, deg			
		ENDOR conformer[a]		
	X-ray	A	B	C
[C(4)–C(3)–C(6)–O(2)]	149		146 ± 5	
[C(4)–C(3)–C(6)–N]	−31		−35 ± 5	
[C(3)–C(6)–N–C^α]	−172		−170 ± 4	
[O(2)–C(6)–N–C^α]	8		9 ± 4	
[C(6)–N–C^α–C^β]	130		144 ± 12	
[C(6)–N–C^α–C]	−107		−93 ± 12	
[N–C^α–C–O′]	−20	120 ± 10	−28 ± 28	−95 ± 15
[N–C^α–C–O″]	163	−57 ± 10	155 ± 28	88 ± 15
[C^β–C^α–C–O′]	103	−118 ± 10	94 ± 28	27 ± 15
[C^β–C^α–C–O″]	−75	65 ± 10	−83 ± 28	−150 ± 15
[C^α–C–O″–C_E]	175	−132 ± 22	−115 ± 40	108 ± 30
[O′–C–O″–C_E]	−3	51 ± 22	68 ± 40	−69 ± 30

[a] Dihedral angles not involving carboxylate atoms are identical for each of the three structures A, B, and C of Figure 8.

of the molecule are again in good agreement with the reference molecular model while there are considerable differences between the values of dihedral angles defining the conformations of the methyl carboxylate group. For the reference compound these differences result from crystal packing effects, as is readily verified, for instance, by comparison of the conformation of the ester group of methyl (benzyloxycarbonyl)-(α-aminoisobutyryl)$_2$-L-alanate[26] to that in the reference tripeptide[10] employed in this investigation. It is, therefore, of interest that the values of the [N–C^α–C–O′], ..., [C^β–C^α–C–O″] dihedral angles of conformer B are nearest to those in the reference compound.

The dihedral angles [C(6)–N–C^α–C] and [N–C^α–C–O″] of the spin-labeled methyl L-alanate compound correspond to the classical ϕ and ψ angles of peptide bonds. In this respect, it is of interest to compare the values of these two dihedral angles to those determined for *N*-acetyl-L-alanine-*N*-methylamide[18d] in solution. Analysis of NMR and circular dichroism spectra shows that the terminal amide linkage exhibits three conformations in solution, corresponding to ϕ,ψ angles characteristic of a right-handed α-helix (−80°, −50°), a polypyroline II like conformation (−80°, 150°), and a 2_7 ribbon conformation (−80°, 80°). As seen in Table III, these dihedral angles are comparable to the values of [C(6)–N–C^α–C] and [N–C^α–C–O″] of conformers A, B, and C, respectively. Thus, each of the conformers identified through torsion angle search calculations as compatible with the ENDOR distance constraints is equivalent to a classical conformation observed in alanyl peptides. It is consequently of immediate importance to evaluate whether the ENDOR data apply to a mixture of all three conformers in solution or whether they apply to a single preferred conformer of the spin-labeled methyl L-alanate molecule.

To predict the preferred conformation of the spin-labeled methyl alanate and to estimate the relative population of each conformer in solution, we have carried out preliminary potential energy calculations with use of force field parameters developed for nitroxyl spin-labels in molecular dynamics simulations.[27] Conformation A was calculated to be of lower energy by 4.7 kcal/mol than conformation C and lower by 0.7 kcal/mol than conformation B.[27] In fact, the energy difference between conformations B (polyproline II) and A (right-handed α-helix) in our calculations is in good agreement with the value of 1.1 kcal/mol as the energy difference between the α_R and polyproline II conformations calculated as the lowest energy conformers of *N*-acetyl-L-alanine-*N*-methylamide in solution.[18e] From these energy differences, it is relatively straightforward to predict that at room temperature 70% of the molecules in solution would be found in conformation

(26) Prasad, B. V.; Shamala, N.; Nagaraj, R.; Balaram, P. *Acta Crystallogr., Sect. B.* **1980**, *36*, 107–110.
(27) Romanowski, H. T.; Makinen, M. W.; van Gunsteren, W. F., unpublished observations.

A while at −100 °C, the freezing point of methanol, the population of the molecules in this conformation increases to ~90%. This result suggests that under the conditions in which solutions of spin-labeled methyl L-alanate were prepared for ENDOR studies the molecules are found predominantly in one conformation and that the ENDOR results, thus, describe primarily a single conformation. It is, therefore, of some interest to note that this conformer designated A in Figure 8 corresponds closest not only to the ϕ,ψ dihedral angles characteristic of a right-handed α-helix but also to the classical Z conformer of an ester group, which is of lower energy than its corresponding E rotamer.[28]

Registry No. I, 125109-37-7; II, 125109-38-8; III, 125137-89-5; IV, 125109-39-9; V, 125109-40-2; VI, 125109-41-3; H-Ala-OH, 56-41-7; L-$H_2NCD(CD_3)COOH$, 18806-29-6; L-$H_2NCD(CH_3)COOH$, 21386-65-2; L-$H_2NCH(CD_3)COOH$, 63546-27-0; H-Ala-OMe·HCl, 2491-20-5; L-$H_2NCD(CD_3)COOMe$·HCl, 125109-42-4; L-$H_2NCD(CH_3)COOCD_3$·HCl, 125109-43-5; L-$H_2NCH(CD_3)COOCD_3$·HCl, 125109-44-6; L-$H_2NCD(CD_3)COOCD_3$·HCl, 125109-45-7; 2,2,5,5-tetramethyl-1-oxypyrroline-3-carboxylic acid, 2154-67-8; 2,2,5,5-($^2H_{12}$)tetramethyl-1-oxy-4-(^2H)pyrroline-3-carboxylic acid, 88168-79-0.

(28) Wiberg, K. B.; Laidig, K. E. *J. Am. Chem. Soc.* **1987**, *109*, 5935-5943.

Structure and Conformation of Spin-Labeled Amino Acids in Frozen Solutions Determined by Electron Nuclear Double Resonance. 2. Methyl *N*-(2,2,5,5-Tetramethyl-1-oxypyrrolinyl-3-carbonyl)-L-tryptophanate, a Molecule with Multiple Conformations[1a]

Gregg B. Wells,[1b] Devkumar Mustafi, and Marvin W. Makinen*

Contribution from the Department of Biochemistry and Molecular Biology, The University of Chicago, Cummings Life Science Center, 920 East 58th Street, Chicago, Illinois 60637.
Received June 7, 1989

Abstract: The conformation of methyl *N*-(2,2,5,5-tetramethyl-1-oxypyrrolinyl-3-carbonyl)-L-tryptophanate in frozen solutions has been determined by application of electron nuclear double resonance (ENDOR) spectroscopy and computer-based molecular modeling. ENDOR spectra of methyl L-tryptophanate and of the corresponding methyl esters of ζ3-fluoro- and η2-fluorotryptophan acylated at the amino group with the spin-label 2,2,5,5-tetramethyl-1-oxypyrroline-3-carboxylic acid exhibited well-resolved resonance adsorptions from protons and fluorines of the amino acid moiety. The ENDOR shifts were shown to correspond to principal hyperfine coupling (hfc) components, from which the dipolar contributions were estimated to calculate electron–nucleus separations. The ENDOR data indicated that there are two distinct conformations of spin-labeled methyl tryptophanate, the relative populations of which were dependent on solvent polarity. Torsion angle search calculations constrained by the ENDOR data showed that the predominant conformation in methanol was similar to that of a classical g^- rotamer ($\chi_1 \sim -63°$) with a near perpendicular ($\chi_2 \sim +105°$) orientation of the indole ring. The second conformer was characterized by $\chi_1 \sim -95°$ and $\chi_2 \sim -105°$, indicative of an antiperpendicular orientation. In chloroform/toluene only the antiperpendicular conformer was detected. The different solvent-dependent orientations of the indole ring with respect to the nitroxyl group are explained on the basis of dipolar interactions of the aromatic side chain with solvent and with the peptide bond.

The structure and conformation of amino acids and peptides in solution are of considerable importance in biophysical studies since the distribution of the side-chain dihedral angles is far from random and preferred conformations of amino acid side chains are frequently observed in proteins.[2] In general, the conformational analysis of amino acid and peptide derivatives in solution has been carried out on the basis of circular dichroism, infrared spectroscopy, nuclear magnetic resonance (NMR[3]), and potential energy calculations. Analysis of direct structural data obtained by NMR methods depends primarily on estimates of the vicinal, through-bond coupling constants of H^α with the peptide amide proton H^N or on estimates of coupling constants of protons bonded to adjacent carbons along the side chain.[4] Reliable estimates of the vicinal coupling constants are difficult to obtain, and the data must be analyzed for multiple conformations, the relative populations of which are not estimated with high precision. In addition, such NMR data are often not analyzed further to determine whether the resonances derive from distinct conformers or whether they derive from multiple conformers that are in rapid equilibrium with each other on the NMR time scale. Also, there are little data to specify internucleus distances on which basis the conformational analysis would be significantly strengthened.

A variety of important problems in chemistry and biochemistry revolve around the relative conformational analysis of molecular structure. To this end we have found that electron nuclear double resonance (ENDOR[3]) spectroscopy can be incisively applied to assign structure and conformation of molecules in solution. In the accompanying publication[5] we demonstrated on the basis of ENDOR and molecular modeling that a nitroxyl spin-labeled derivative of L-alanine exhibits only one preferred conformation. In this communication we extend this approach to investigate the conformational properties of L-tryptophan, an amino acid that is expected to exhibit multiple conformations in solution.[6,7] We

(1) (a) This work was supported by a grant from the National Institutes of Health (GM 21900). (b) Supported in part by an MSTP Training Grant from the National Institutes of Health (GM 07281).

(2) (a) Chandrasekaran, R.; Ramachandran, G. N. *Int. J. Protein Res.* **1970**, *2*, 223-233. (b) Chothia, C. *Annu. Rev. Biochem.* **1984**, *53*, 537-572.

(3) The following abbreviations are used: EPR, electron paramagnetic resonance; ENDOR, electron nuclear double resonance; hf, hyperfine; hfc, hyperfine coupling; NMR, nuclear magnetic resonance; rf, radio frequency.

(4) (a) Feeney, J. *Proc. R. Soc. London, A* **1975**, *345*, 61-72. (b) Wüthrich, K. *NMR of Proteins and Nucleic Acids*; John Wiley & Sons: New York, 1986; p 292. (c) Wüthrich, K. *Acc. Chem. Res.* **1989**, *22*, 36-44.

(5) Mustafi, D.; Sachleben, J. R.; Wells, G. B.; Makinen, M. W. *J. Am. Chem. Soc.*, preceding article in this issue.

0002-7863/90/1512-2566$02.50/0